



**AIAA 2006-1891**

**CHARGE DETERMINATION FOR  
SPECIFIED SHAPE COULOMB  
FORCE VIRTUAL STRUCTURES**

Gordon G. Parker, Lyon B. King

*Michigan Technological University, Houghton, MI 49931*

and Hanspeter Schaub

*Virginia Tech, Blacksburg, VA 24061*

**47th AIAA/ASME/ASCE/AHS/ASC Structures,  
Structural Dynamics, and Materials Conference  
May 1–4, 2006, Newport, Rhode Island**

# Charge Determination for Specified Shape Coulomb Force Virtual Structures

Gordon Parker\* and Lyon King\*

*Michigan Technological University, Houghton, MI, 49931, USA*

Hanspeter Schaub†

*Virginia Tech, Blacksburg, VA, 24061, USA*

The focus of this paper is the generation of high Earth orbit (HEO) Coulomb force structures. These structures are characterized by a set of charge carrying nodes, but no interconnecting struts. By correctly setting the node charges, the inter-node Coulomb forces create a static, crystal-like structure. The uniqueness of the work is the examination of how to form *specified* shape structures using a subset of all available nodes. In addition, the plasma shielding effect is considered explicitly. An equilateral triangle structure example is given to illustrate the approach where 5 nodes are used in the structure, 3 of which used to satisfy the equilateral triangle shape goal. The example also illustrates that practical Coulomb structures should have inter-node separation distances in the 10s of meters range or less.

## I. Introduction

Coulomb force structures are a relatively new concept consisting of several electrostatically chargeable nodes with no interconnecting struts. Instead, the node charges are carefully controlled so that the net structure is held together solely by the Coulomb forces generated between all the nodes. This ‘virtual structure’ can also be considered as a free-flying, constant-shape formation of several spacecraft. Advantages of Coulomb force virtual structures include low mass, low propellant usage, reconfigurability, and self-assembly. Large virtual structures on the order of 20–100 meters are envisioned where controlled electrostatic force fields are used to bond the individual craft into a single structure. By changing control laws, it will be possible to increase or decrease the stiffness or flexibility of sub-components, or even change the size and shape of the overall structure. This will allow for highly reconfigurable structures which can adapt to changing mission needs. Disadvantages also exist including control system complexity, restriction to high Earth orbits (HEO) and deep space missions due to charge shielding at lower orbits, and ensuring that the charged nodes are electrically isolated to minimize differential charge effects.

The earliest work in this area examined symmetric structures where one node had a conventional propulsion system.<sup>4,8–10</sup> This allowed the other nodes to react against a body that was maintaining a constant orbit. The report in Reference 10, using data from the SCATHA<sup>11</sup> and ATS<sup>6</sup> missions, showed that  $10\mu N$ – $1000\mu N$  level forces could be generated between nodes. In addition, charging times were estimated to be in the millisecond range, and the Coulomb ‘thrust’ propulsion system power consumption was lower than for conventional propulsion methods. More recent work has examined the necessary conditions for static equilibrium where all nodes are held together by Coulomb forces alone.<sup>12,13</sup> Multiple node, free-flying structures were considered in detail for 2 and 3 node cases.<sup>1</sup> This was followed by consideration of larger structures using a genetic algorithm optimization strategy to find static shapes for up to 9 nodes<sup>2</sup> where the plasma shielding effect, characterized by the Debye length, was considered negligible.

The remainder of this paper’s content is as follows. The Coulomb structure’s orbital dynamic and static equilibrium equations are given in Section II, in addition to a convenient normalized form suitable for charge

---

\*Associate Professor, Mechanical Engineering - Engineering Mechanics Dept., 1400 Townsend Dr., Houghton MI 49931, and AIAA Member Grade.

†Assistant Professor, Aerospace & Ocean Engineering Dept., Address, and AIAA Member Grade.

calculation independent of several physical parameters. Section III illustrates the optimization approach used for computing node charges, with an example provided in Section IV. A few concluding remarks are given in Section V.

## II. Normalized Virtual Structure Model

Before examining the virtual structure equilibrium charge equations, the Coulomb charge, voltage and force relationships should be discussed. It's well known that Coulomb forces exist between charged bodies. Considering the two charged spheres of Figure 1 the Coulomb force magnitude acting on body 1, directed along the line between the spheres, is

$$f_{12} = \frac{k_c q_1 q_2}{d^2} \quad (1)$$

where  $k_c$  is Coulomb's constant ( $8.99 \times 10^9 \frac{Nm^2}{C^2}$ ),  $q_1$  and  $q_2$  are the node charges in Coulombs and  $d$  is the distance between the center of the spherical nodes in meters.

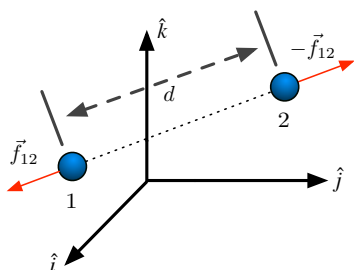


Figure 1. Coulomb forces between two spheres.

An important deviation from the ideal Coulomb force model of Eq. 1 occurs when considering charged bodies in a plasma-rich environment, as found in space. In short, the plasma shields the Coulomb force effect exponentially with the separation distance as shown in Eq. 2. The exponential decay of the Coulomb force is characterized by the Debye length,  $\lambda_d$ , which varies with plasma characteristics.<sup>3</sup> In general, the Debye length is small at LEO and large at HEO (roughly 10 cm and 100 m respectively).

$$f_{12} = \frac{k_c q_1 q_2}{d^2} e^{-d/\lambda_d} \quad (2)$$

When nodes are more than 2 Debye length apart, then their Coulomb force interaction becomes negligible for realistic charge scenarios. This generally negative feature is not without potential applications. Debye shielding decoupling between subsets of the structure may simplify eventual control design. Finally, it should be noted that the charges can be converted to voltages for the  $i$ th node, which may give more practical insight, according to

$$V_i = \frac{q_i k_c}{r_n} \quad (3)$$

where  $r_n$  is the node radius and the nodes are assumed to be spherical.

Next, Hill's equations<sup>7</sup> (also known as the Clohessy-Wiltshire equations,<sup>5</sup>) are used to generate the static equilibrium equations for the Coulomb virtual structure. The standard equations are in terms of several physical parameters (separation distances, charges, node radii, etc.). A normalized form of the Coulomb structure equations is created to reduce the number of parameters, thus allowing families of solutions to be created from a single normalized equation solution.

Consider  $N$  virtual structure nodes such that their center of mass is in a circular orbit about the Earth, such as the 3-node example of Figure 2. The Hill coordinate frame has its origin at the structure's center of mass with the  $\hat{i}$  unit vector pointing radially outward from the center of the Earth. The  $\hat{j}$  axis is in the direction of the center of mass velocity vector. Each node, numbered 1 through  $N$ , is assumed to be a homogeneously charged sphere. In general, the  $i$ th node has its own charge,  $q_i$ , and a relative position vector from the origin of the Hill frame to the center of the node, denoted  $\mathbf{p}_i$ . Each position vector has elements  $x_i$ ,  $y_i$  and  $z_i$ .

Setting the speed and acceleration terms in Hill's equations to zero, and applying the Coulomb forces to

the right side, yields the Coulomb structure equilibrium equations

$$\begin{aligned}
-3n^2 x_i &= \frac{k_c}{m} \sum_{j=1}^N \frac{x_i - x_j}{|\mathbf{p}_i - \mathbf{p}_j|^3} q_i q_j e^{-|\mathbf{p}_i - \mathbf{p}_j|/\lambda_d} \\
0 &= \frac{k_c}{m} \sum_{j=1}^N \frac{y_i - y_j}{|\mathbf{p}_i - \mathbf{p}_j|^3} q_i q_j e^{-|\mathbf{p}_i - \mathbf{p}_j|/\lambda_d} \quad i \neq j \\
n^2 z_i &= \frac{k_c}{m} \sum_{j=1}^N \frac{z_i - z_j}{|\mathbf{p}_i - \mathbf{p}_j|^3} q_i q_j e^{-|\mathbf{p}_i - \mathbf{p}_j|/\lambda_d}
\end{aligned} \tag{4}$$

where  $n$  is the Hill frame angular velocity, and  $m$  is the mass of a node where all nodes are assumed to have the same size and mass.

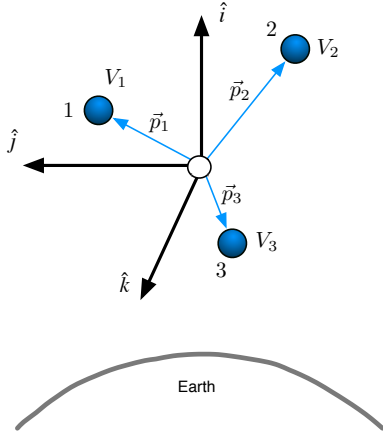


**Figure 2.** Three virtual structure nodes orbiting the Earth illustrating the notation used in the model development.

To start the nondimensionalization process, divide both sides of Eq. 4 by  $n^2$  and rearrange

$$\begin{aligned}
-3x_i &= \sum_{j=1}^N \frac{x_i - x_j}{|\mathbf{p}_i - \mathbf{p}_j|^3} \left( \frac{r_n}{n\sqrt{mk_c}} V_i \right) \left( \frac{r_n}{n\sqrt{mk_c}} V_j \right) e^{-|\mathbf{p}_i - \mathbf{p}_j|/\lambda_d} \\
0 &= \sum_{j=1}^N \frac{y_i - y_j}{|\mathbf{p}_i - \mathbf{p}_j|^3} \left( \frac{r_n}{n\sqrt{mk_c}} V_i \right) \left( \frac{r_n}{n\sqrt{mk_c}} V_j \right) e^{-|\mathbf{p}_i - \mathbf{p}_j|/\lambda_d} \\
z_i &= \sum_{j=1}^N \frac{z_i - z_j}{|\mathbf{p}_i - \mathbf{p}_j|^3} \left( \frac{r_n}{n\sqrt{mk_c}} V_i \right) \left( \frac{r_n}{n\sqrt{mk_c}} V_j \right) e^{-|\mathbf{p}_i - \mathbf{p}_j|/\lambda_d}
\end{aligned} \tag{5}$$

where Eq. 3 has been used to convert the inputs from charges to voltages. Next, define nondimensional position coordinates as

$$\begin{aligned}
\tilde{x}_i &= \frac{x_i}{M\lambda_d} \\
\tilde{y}_i &= \frac{y_i}{M\lambda_d} \\
\tilde{z}_i &= \frac{z_i}{M\lambda_d}
\end{aligned} \tag{6}$$

where  $M$  is the number of Debye lengths, and defines the characteristic length used for nondimensionalization. For example, to nondimensionalize using 1.5 Debye lengths, let  $M = 1.5$ . Applying this to Eq. 5 yields the final set of nondimensional, static equilibrium, Coulomb structure equations of Eq. 7.

$$\begin{aligned}
-3\tilde{x}_i &= \sum_{j=1}^N \frac{\tilde{x}_i - \tilde{x}_j}{|\tilde{\mathbf{p}}_i - \tilde{\mathbf{p}}_j|^3} \tilde{V}_i \tilde{V}_j e^{-M|\tilde{\mathbf{p}}_i - \tilde{\mathbf{p}}_j|} \\
0 &= \sum_{j=1}^N \frac{\tilde{y}_i - \tilde{y}_j}{|\tilde{\mathbf{p}}_i - \tilde{\mathbf{p}}_j|^3} \tilde{V}_i \tilde{V}_j e^{-M|\tilde{\mathbf{p}}_i - \tilde{\mathbf{p}}_j|} \\
\tilde{z}_i &= \sum_{j=1}^N \frac{\tilde{z}_i - \tilde{z}_j}{|\tilde{\mathbf{p}}_i - \tilde{\mathbf{p}}_j|^3} \tilde{V}_i \tilde{V}_j e^{-M|\tilde{\mathbf{p}}_i - \tilde{\mathbf{p}}_j|}
\end{aligned} \tag{7}$$

where  $\tilde{\mathbf{p}}_i = [\tilde{x}_i \ \tilde{y}_i \ \tilde{z}_i]^T$  and

$$\tilde{V}_i = \frac{r_{s/c}}{n\sqrt{m(M\lambda_d)^3 k_c}} V_i \tag{8}$$

Finding a charge/position set (i.e.  $\tilde{\mathbf{p}}_i, \tilde{V}_i, \quad i = 1 \dots N$ ) that satisfies Eq. 7 for a specified Debye length fraction ( $M$ ) yields a family of Coulomb force structures for any altitude (or circular orbit speed  $n$ ), node

radius ( $r_n$ ), node mass ( $m$ ) and plasma Debye length ( $\lambda_d$ ). The Hill frame angular velocity,  $n$ , can be found from circular orbit analysis

$$n = \sqrt{\frac{\mu}{r^3}} \quad (9)$$

where  $\mu$  is the standard gravitational parameter for Earth ( $\mu \approx 3.986 \times 10^{14} \frac{m^3}{s^2}$ ) and  $r$  is the circular orbit radius. Although  $n$  can be readily computed from Eq. 9, Table 1 shows these values for various  $r$  as a quick reference along with estimates of the altitude dependent Debye lengths.

| Altitude (km) | Radius (m)         | Period (hr) | Speed (m/s) | n (rad/s)             | Appx. $\lambda_d$ (m) |
|---------------|--------------------|-------------|-------------|-----------------------|-----------------------|
| 300           | $6.68 \times 10^6$ | 1.51        | 7720        | $116 \times 10^{-5}$  | 0.01-0.03             |
| 500           | $6.88 \times 10^6$ | 1.58        | 7610        | $111 \times 10^{-5}$  | 0.01-0.03             |
| 2000          | $8.38 \times 10^6$ | 2.12        | 6900        | $82.3 \times 10^{-5}$ | 0.03-0.26             |
| 10000         | $16.4 \times 10^6$ | 5.81        | 4930        | $30.1 \times 10^{-5}$ | 0.03-0.26             |
| 35800         | $42.2 \times 10^6$ | 24.0        | 3070        | $7.28 \times 10^{-5}$ | 75-575                |

Table 1. Speed information as a function of circular orbit altitude.

### III. Node Charge Calculation

In general, a desired Coulomb structure shape cannot be realized with the minimum number of nodes needed to create a conventional truss structure. For example, to create a box in a circular orbit with one plane always orthogonal to the Earth radial direction, a minimum of 8 nodes is required for a conventional structure. If in addition its principal inertia axes are orientated with its Hill frame axes, it will maintain this orientation during its orbit (neglecting perturbations due to aerodynamic forces,  $J_2$  gravitational effects, solar radiation, etc.). Due to the force interaction between all the nodes of a Coulomb force structure, in general, it is not possible to form a structure with the minimum number of nodes. Additional nodes are required to ensure that static equilibrium is achieved when simultaneously considering the Coulomb and gravitational forces.

The approach described below assumes that a fixed number of node assets are available for creating the structure that is larger than the minimum number needed to create a conventional structure. An optimization process is then used to compute the charge/position set for all the nodes that solves Eq. 7 while ensuring that the shape is attained by the minimum number of nodes needed to form the conventional structure. It should be noted that an analytical method for determining the minimum number of Coulomb nodes given a specified shape does not exist as yet.

The use of an optimization code to select design parameters, in this case node charges and locations, is nothing new. The interesting aspect of the implementation is the cost function where shape and equilibrium equation constraints are imposed as penalty terms. The cost function used in this study, and that gives reliable convergence to a solution when using a gradient based optimization scheme, is shown in Eq. 10

$$J = \left( \frac{\max |\tilde{V}_i|}{\min |\tilde{V}_i|} \right) \sum_{i=1}^N |\tilde{\mathbf{R}}_i| + w_1 S(\tilde{\mathbf{p}}_i, \mathbf{L}_p) + w_2 \{ |I_{xy}| + |I_{xz}| + |I_{yz}| \} \quad (10)$$

where  $w_1$  and  $w_2$  are weighting coefficients that shift emphasis between the three main terms of  $J$ . The  $R_i$  are the residuals corresponding to inexact solution to Eq. 7 and are given by

$$\tilde{\mathbf{R}}_i = \begin{bmatrix} 3\tilde{x}_i + \sum_{j=1}^N \frac{\tilde{x}_i - \tilde{x}_j}{|\tilde{\mathbf{p}}_i - \tilde{\mathbf{p}}_j|^3} \tilde{V}_i \tilde{V}_j e^{-M|\tilde{\mathbf{p}}_i - \tilde{\mathbf{p}}_j|} \\ \sum_{j=1}^N \frac{\tilde{y}_i - \tilde{y}_j}{|\tilde{\mathbf{p}}_i - \tilde{\mathbf{p}}_j|^3} \tilde{V}_i \tilde{V}_j e^{-M|\tilde{\mathbf{p}}_i - \tilde{\mathbf{p}}_j|} \\ -\tilde{z}_i + \sum_{j=1}^N \frac{\tilde{z}_i - \tilde{z}_j}{|\tilde{\mathbf{p}}_i - \tilde{\mathbf{p}}_j|^3} \tilde{V}_i \tilde{V}_j e^{-M|\tilde{\mathbf{p}}_i - \tilde{\mathbf{p}}_j|} \end{bmatrix} \quad (11)$$

The positive, scalar function  $S$  is zero only when the desired shape is attained. It is in general a function of the relative position vectors, and a set of shape defining parameters contained in  $\mathbf{L}_p$ .  $I_{xy}$ ,  $I_{xz}$ , and  $I_{yz}$

are the products of inertia of the structure, and are a function of the  $\tilde{\mathbf{p}}_i$ . The first term of Eq. 10 penalizes any configuration that does not satisfy the fundamental Coulomb structure, static equilibrium equations, while ensuring that charge is shared amongst the participating nodes. The second term focuses on creation of the desired shape. The third term favors alignment of the structure’s principal axes with the Hill frame. This promotes the satisfaction of Eq. 7 since these are necessary conditions for static equilibrium. Although the Debye length shielding is considered in the residuals, its effect is usually relatively small as long as the distances between craft are within 1 Debye length.

The center of mass constraint,  $\tilde{\mathbf{p}}_{cm} = \mathbf{0}$  is enforced directly through the selection of free optimization parameters. Rather arbitrarily, the  $N$ th node’s position vector,  $\tilde{\mathbf{p}}_N$  is not allowed to be free, but is instead computed to enforce the constraint. In general the optimization problem can be stated as: find the  $4N - 3$  parameters ( $\tilde{\mathbf{p}}_i, i = 1 \dots N - 1$  and  $\tilde{V}_i, i = 1 \dots N$ ) such that Eq. 10 is minimized.

## IV. Example

The shape goal is to create a structure that when projected onto the  $y - z$  Hill frame, forms an equilateral triangle. It should be noted that the nodes of the equilateral triangle need not lie in this plane, but as viewed from Earth, one would see the desired equilateral triangle shape. The minimum number of nodes is 3, with the total number of node assets chosen as  $N = 5$ . Since the center of mass constraint is satisfied directly, there are 17 free parameters - the position vectors of nodes 1-4 and the voltages of all 5 nodes.

The cost function, with the shape goal function  $S$  specified is given in Eq. 12

$$J = \left( \frac{\max |\tilde{V}_i|}{\min |\tilde{V}_i|} \right) \sum_{i=1}^5 |\tilde{\mathbf{r}}_i| + w_1 \left\{ \left| \text{Proj}_{\hat{y}, \hat{z}} (\tilde{\mathbf{p}}_2 - \tilde{\mathbf{p}}_1) - \tilde{L}_p \right| + \right. \\ \left. \left| \text{Proj}_{\hat{y}, \hat{z}} (\tilde{\mathbf{p}}_2 - \tilde{\mathbf{p}}_3) - \tilde{L}_p \right| + \left| \text{Proj}_{\hat{y}, \hat{z}} (\tilde{\mathbf{p}}_3 - \tilde{\mathbf{p}}_1) - \tilde{L}_p \right| \right\} + \\ w_2 \left\{ |I_{xy}| + |I_{xz}| + |I_{yz}| \right\} \quad (12)$$

where  $\tilde{L}_p$  is the normalized equilateral side length. The penalty function weights,  $w_1$  and  $w_2$  were both chosen as 10.0 throughout the remainder of the example.

The solution for  $M = 1$  and  $\tilde{L}_p = 0.5$  is used to illustrate a typical solved structure shape. The nondimensional node charges are shown in Table 2.

A view from Earth and a perspective view are given in Figure 3 and Figure 4. The color bar is the nondimensional voltage magnitude as a percent of the maximum normalized voltage,  $\tilde{V}_{\max} = 1.6398$ . Since the nondimensional separation distance was set to 0.5 and  $M = 1$ , the actual equilateral triangle separation distance (between craft 1,2,3) in meters is

$$L_p = .5\lambda_d \quad (13)$$

Thus, a family of solutions has been created for any altitude dependent Debye length where at higher altitudes the triangle side length becomes larger.

Charge/shape solutions were obtained for several values of  $M$ . Table 3 shows the results of converting nondimensional, maximum node voltages back to true voltages for a variety of altitudes, Debye lengths, and equilateral triangle separation distances. This illustrates that to obtain ‘reasonable’ equilateral node separation distances, the structure should exploit the large Debye lengths at GEO. If node voltages must stay in the 10,000 volt range, then equilateral separation distances of about 10 meters are feasible.

Figure 5 Shows the maximum true node voltage as a function of both Debye length and the  $L_p/\lambda_d$  ratio. The absolute voltage levels can be extracted from the log scale color bar at the right of the plot. For example, for a  $\lambda_d = 50$  meters, and an  $L_p = 50$  meters, the maximum voltage is approximately  $V_{max} = 10^{5.4} = 250,000$  volts. Figure 5 shows that node voltage requirements increase faster, with increasing equilateral separation

| Node | $\tilde{V}_i$ |
|------|---------------|
| 1    | 1.2840        |
| 2    | -0.7583       |
| 3    | -0.7583       |
| 4    | 0.8841        |
| 5    | 1.6398        |

**Table 2. Nondimensional node voltages for a 5 node structure, with  $M = 1$  and the nondimensional, equilateral triangle separation distance of  $\tilde{L}_p = 0.5$ .**

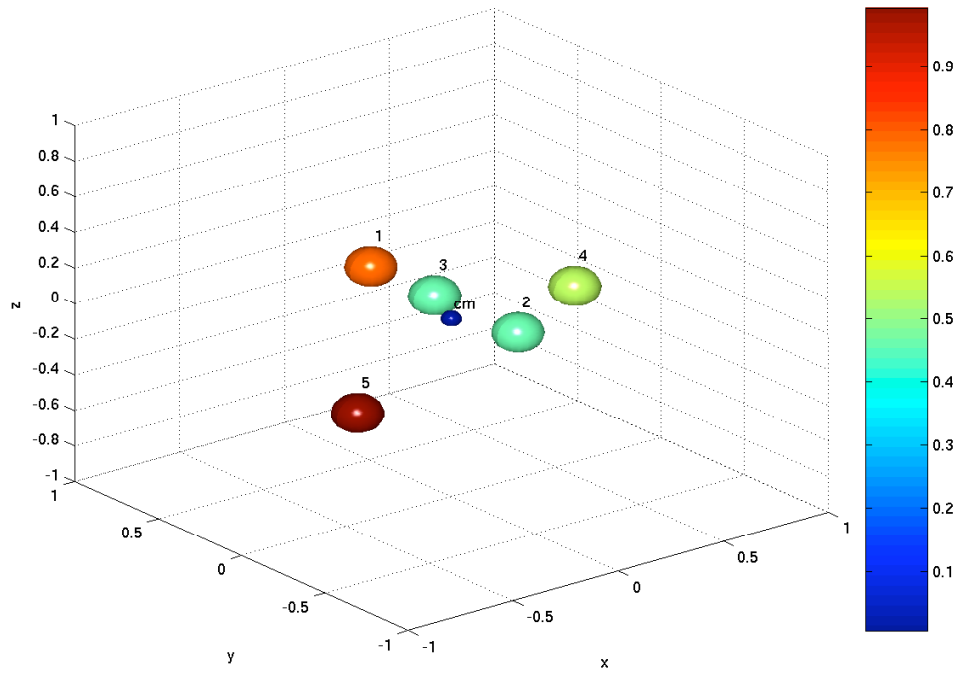


Figure 3. 5 node structure - perspective view. The structure center of mass is shown as a small blue sphere, but of course, has no voltage associated with it.

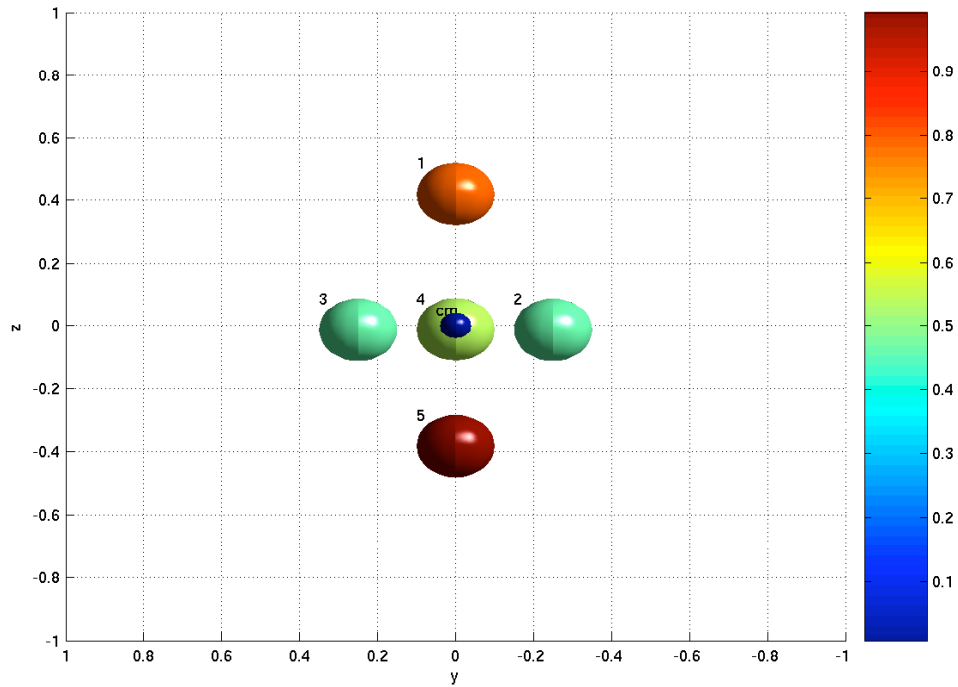


Figure 4. 5 node structure - view from Earth. The structure center of mass is shown as a small blue sphere, but of course, has no voltage associated with it.

| Altitude (km) | $\lambda_d$ (m) | $L_p$ (m) | $V_{max}$ |
|---------------|-----------------|-----------|-----------|
| 300           | .01             | .005      | 2.50      |
|               |                 | .01       | 10.5      |
|               |                 | .02       | 60.9      |
| 10000         | .05             | .025      | 7.30      |
|               |                 | .05       | 30.5      |
|               |                 | .1        | 177       |
| 35800         | 20              | 10        | 14,100    |
|               |                 | 20        | 59,000    |
|               |                 | 40        | 343,000   |
|               | 50              | 12        | 16,100    |
|               |                 | 25        | 55,700    |
|               |                 | 50        | 233,000   |

**Table 3. True node voltages for a variety of altitudes, Debye lengths, and equilateral triangle separation distances.**

distance ratio, when the Debye length is larger. This is because the inverse square separation distance voltage effect is quite significant at large absolute node separation distances such as occur in the upper right quadrant (HEO structures with large node separation, 100-200 m). The lower right quadrant (HEO structures with small separation, 10 m) require relatively small voltages compared to what is possible with very little power consumption.<sup>8</sup>

## V. Conclusions

A method has been presented for generating Coulomb structures with a specified shape. Due to the equation normalization, families of solutions can be inferred from a single optimization result. From a practical perspective, the node voltages become excessive when node separations are more than 0.3-1.0 Debye lengths, depending on the actual Debye length value. At GEO, this is roughly 10 meters. Future work will focus on creating larger structures using more node assets. This should result in a denser ‘packing’ of the nodes, allowing higher forces with smaller charges, and thus larger overall structures.

## VI. Acknowledgments

This work was supported by the U.S. Defense Advance Research Projects Agency (DARPA), Special Projects Office (SPO) under contract number HR0011-05-C-0026. Approved for public release with unlimited distribution.

## References

- <sup>1</sup>John Berryman and Hanspeter Schaub. Analytical charge analysis for 2- and 3-craft coulomb formations. In *AAS/AIAA Astrodynamics Specialist Conference*, Lake Tahoe, CA, August 7–11 2005. Paper No. AAS 05–278.
- <sup>2</sup>John Berryman and Hanspeter Schaub. Static equilibrium configurations in geo coulomb spacecraft formations. In *AAS Spaceflight Mechanics Meeting*, Copper Mountain, CO, Jan. 23–27 2005. Paper No. AAS 05–104.
- <sup>3</sup>F. F. Chen. *Plasma Physics and Controlled Fusion Volume 1: Plasma Physics*, chapter 1. Plenum Press, 1984.
- <sup>4</sup>J.-H. Chong. Dynamic behavior of spacecraft formation flying using coulomb forces. Master’s thesis, Michigan Technological University, 2002.
- <sup>5</sup>W. H. Clohessy and R. S. Wiltshire. Terminal guidance system for satellite rendezvous. *Journal of the Aerospace Sciences*, 27(9):653–658, September 1960.
- <sup>6</sup>H. B. Garrett and S. E. DeFrost. An analytical simulation of the geosynchronous plasma environment. *Planetary Space Science*, 27:1101–1109, 1979.
- <sup>7</sup>G. W. Hill. Researches in the lunar theory. *American Journal of Mathematics*, 1(1):5–26, 1878.



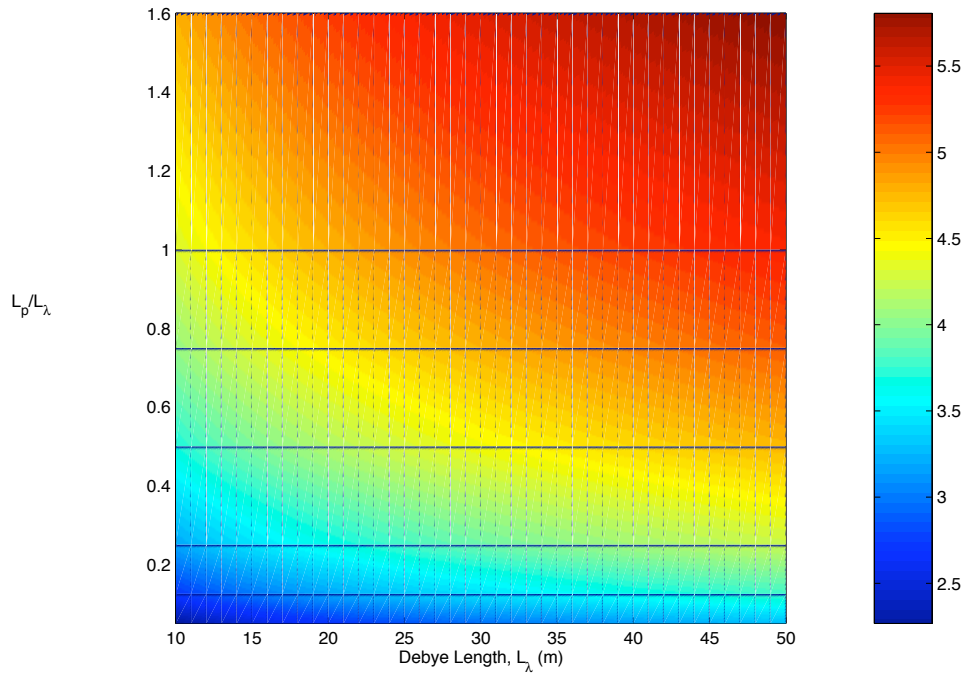


**Figure 5.** Maximum node voltages needed to maintain craft 1,2,3 in an equilateral triangle. The color bar is on a log scale, therefore 2.5 corresponds to  $10^{2.5}$  volts and 6.5 corresponds to  $10^{6.5}$  volts.

<sup>8</sup>Lyon B. King, Gordon G. Parker, and J.-H. Chong. Coulomb controlled spacecraft formation flying. *AIAA Journal of Propulsion and Power*, 19(3):497–505, 2003.

<sup>9</sup>Lyon B. King, Gordon G. Parker, Satwik Deshmukh, and J.-H. Chong. A study of inter-spacecraft coulomb forces and implications for formation flying. In *38th AIAA/ASME/SAE/ASEE Joint Propulsion Conference and Exhibit*, Indianapolis, IN, July 2002. AIAA Paper No. 2002-3671.

<sup>10</sup>Lyon B. King, Gordon G. Parker, Satwik Deshmukh, and Jer-Hong Chong. Spacecraft formation-flying using inter-vehicle coulomb forces. Technical report, NASA Institute for Advanced Concepts, <http://www.niac.usra.edu/studies>, 2002.

<sup>11</sup>E. G. Mullen, M. S. Gussenhoven, and D. A. Hardy. Scatha survey of high-voltage spacecraft charging in sunlight. *Journal of the Geophysical Sciences*, 91:1074–1090, 1986.

<sup>12</sup>Hanspeter Schaub, Christopher Hall, and John Berryman. Necessary conditions for circularly-restricted static coulomb formations. In *AAS Malcolm D. Shuster Astronautics Symposium*, Buffalo, NY, June. 12–15 2005. Paper No. AAS 05–472.

<sup>13</sup>Hanspeter Schaub, Gordon G. Parker, and Lyon B. King. Challenges and prospects of coulomb satellite formation flying. In *AAS John L. Junkins Astrodynamics Symposium*, College Station, TX, May 2003. AAS Paper No. AAS03-278.